PCCP

Accepted Manuscript

ROYAL SOCIETY OF CHEMISTRY

www.rsc.org/pccp

Chemistry in One Dimension

Pierre-François Loos,* Caleb J. Ball, and Peter M. W. Gill†

Research School of Chemistry, Australian National University, Canberra ACT 0200, Australia

Abstract

We report benchmark results for one-dimensional (1D) atomic and molecular systems interacting via the Coulomb operator $|x|^{-1}$. Using various wavefunction-type approaches, such as Hartree-Fock theory, second- and third-order Møller-Plesset perturbation theory and explicitly correlated calculations, we study the ground state of atoms with up to ten electrons as well as small diatomic and triatomic molecules containing up to two electrons. A detailed analysis of the 1D helium-like ions is given and the expression of the high-density correlation energy is reported. We report the total energies, ionization energies, electron affinities and other physical properties of the many-electron 1D atoms and, using these results, we construct the 1D analog of Mendeleev's periodic table. We find that the 1D periodic table contains only two groups: the alkali metals and the noble gases. We also calculate the dissociation curves of several 1D diatomics and study the chemical bond in H_2^+, HeH^{2+}, He_2^{3+}, H_2, HeH^+ and He_2^{2+}. We find that, unlike their 3D counterparts, 1D molecules are primarily bound by one-electron bonds. Finally, we study the chemistry of H_3^+ and we discuss the stability of the 1D polymer resulting from an infinite chain of hydrogen atoms.

PACS numbers: 31.15.A-, 31.15.V-, 31.15.xt

Keywords: one-dimensional atom; one-dimensional molecule; one-dimensional polymer; helium-like ions

* Corresponding author: pf.loos@anu.edu.au

† peter.gill@anu.edu.au

I. 1D CHEMISTRY

Chemistry in one dimension (1D) is interesting for many experimental and theoretical reasons, but also in its own right. Experimentally, quasi-1D systems can be realized in carbon nanotubes [1–5], organic conductors [6–10], transition metal oxides [11], edge states in quantum Hall liquids [12–14], semiconductor heterostructures [15–19], confined atomic gases [20–22] and atomic or semiconducting nanowires. Theoretically, Burke and coworkers [23, 24] have shown that 1D systems can be used as a "theoretical laboratory" to study strong correlation in "real" three-dimensional (3D) chemical systems within density-functional theory [25]. Herschbach and coworkers calculated the ground-state electronic energy of 3D systems by interpolating between exact solutions for the limiting cases of 1D and infinite-dimensional systems [26–28].

However, all these authors eschewed the Coulomb operator $1/|x|$. For example, Burke and coworkers [23, 24] used a softened version of the Coulomb operator $1/\sqrt{x^2+1}$ to study 1D chemical systems, such as light atoms (H, He, Li, Be, ...), ions (H^-, Li^+, Be^+, ...), and diatomics (H_2^+ and H_2). Herschbach and coworkers have worked intensively on the 1D He atom [29–32] replacing the usual Coulomb inter-particle interaction with the Dirac delta function $\delta(x)$ [33–36]. There are few studies using the Coulomb operator because of its strong divergence at $x = 0$. Most of these focus on non-atomic and non-molecular systems [37–43].

In this manuscript, we develop a consistent and systematic framework for examining electron correlation within simple models that involve only one spatial coordinate. We prefer the Coulomb operator because, although it is not the solution of the 1D Poisson equation, it pertains to particles that are restricted to a *1D sub-space of 3D space*. We refrain from modifying this operator, for example by softening the singularity or using harmonic potentials to create the linear confinement, as this can have dramatic effects upon the behaviour that we seek to study [41]. Furthermore, such modifications typically require a parameter to describe the extent to which they differ from the original operator, thereby unhelpfully complicating the analysis.

The first 1D chemical system to be studied was the H atom by Loudon [44]. Despite its simplicity, this model has been useful for studying the behavior of many physical systems, such as Rydberg atoms in external fields [45, 46] or the dynamics of surface-state electrons in liquid helium [47, 48] and its potential application to quantum computing [49, 50]. Most work

since Loudon has focused on one-electron ions [44, 51–57] and, to the best of our knowledge, no calculation has been reported for larger chemical systems.

In part, this can be attributed to the ongoing controversy concerning the mathematical structure of the problem. The nature of the appropriate eigenfunctions, namely their parity and boundedness, has generated much debate in the past [57–64]. At the same time there has been significant work on the appropriate boundary conditions (or, equivalently, the self-adjoint extension) for the problem [65–68]. In the present work we assume, based upon recent publications by a number of authors [57, 67–69], that the Coulomb potential gives rise to impenetrable nuclei. We discuss this further in Sec. III.

In Sec. III and Sec. IV, we report electronic structure calculations for 1D atomic and molecular systems using the unadorned Coulomb operator $1/|x|$. Sec. IV discusses several diatomic systems, the chemistry of H_3^+ and an infinite chain of 1D hydrogen atoms.

Because of the singularity of the Coulomb interaction in 1D, the electronic wavefunction has nodes [70] at all points where two electrons touch [71]. As a result, all 1D systems are spin-blind [37–39, 41] and we are free to assume that all electrons have the same spin. This also means that the Pauli exclusion principle forbids *any* two electrons in 1D to have the same quantum state and, in independent-electron models such as Hartree-Fock (HF) theory [72], orbitals have a maximum occupancy of one.

Unless otherwise stated, atomic units are used throughout: total energies in hartrees (E_h), correlation energies in millihartrees (mE_h) and bond lengths in bohrs.

II. THEORY

A. Notation

Because of the impenetrability of the Coulomb operator [57, 62, 69] (see Sec. III), electrons cannot pass from one side of a nucleus to the other and are trapped in domains which are either rays (to the left or right of the molecule) or line segments (between nuclei).

The resulting domain occupations lead to families of states which can be defined by specifying the occupied orbitals in each domain. For example, the notation ${}_i\mathrm{A}_j^{Z_\mathrm{A}-2}$ denotes an atom A of nuclear charge Z_A whose ith left orbital and jth right orbitals are (singly) occupied. Likewise, $\mathrm{A}_{i,j}^{Z_\mathrm{A}-2}$ indicates an atom with two electrons, in the ith and jth orbitals,

on the right side of the nucleus. 1D molecules can be similarly described. For example, $A_{1,4}B_1^{Z_A+Z_B-3}$ denotes a diatomic in which two electrons are between the nuclei and one electron is on the B side of the molecule. When consecutive orbitals are occupied in the same domain, we use dashes. For example, $A_{1-3}B^{Z_A+Z_B-3}$ implies that the three lowest orbitals between the nuclei are occupied.

B. Computational details

We have followed the methods developed by Hylleraas [73, 74] and James and Coolidge [75] to compute the exact or near-exact energies E_{exact} of one-, two-, and three-electron systems. We have written a standalone program [76] called CHEM1D to perform HF and Møller-Plesset perturbation theory calculations [72] on arbitrary 1D atomic and molecular systems.

All our atomic and molecular calculations use a normalized basis of exponentials on the ray to the left of the leftmost nucleus,

$$\mathcal{L}_k^A(x) = 2k^3\alpha^{3/2}(A-x)e^{-k^2\alpha(A-x)}, \tag{1}$$

exponentials on the ray to the right of the rightmost nucleus,

$$\mathcal{R}_k^B(x) = 2k^3\alpha^{3/2}(x-B)e^{-k^2\alpha(x-B)}, \tag{2}$$

even polynomials on the line segment between adjacent nuclei,

$$\mathcal{E}_k^{AB}(x) = \sqrt{\frac{2/\pi^{1/2}}{R_{AB}}\frac{\Gamma(2k+3/2)}{\Gamma(2k+1)}}\,(1-z^2)^k, \tag{3}$$

and odd polynomials on the line segment between adjacent nuclei,

$$\mathcal{O}_k^{AB}(x) = \sqrt{\frac{4/\pi^{1/2}}{R_{AB}}\frac{\Gamma(2k+5/2)}{\Gamma(2k+1)}}\,z(1-z^2)^k, \tag{4}$$

where $z = (A+B-2x)/(A-B)$, $R_{AB} = |A-B|$ and Γ is the Gamma function [77]. By including only positive integer k, we ensure that the orbitals vanish at the nuclei. Some of

these basis functions are shown in Fig. 1. Full details of these calculations will be reported elsewhere [76].

The HF eigenvalues and orbitals yield [72] the second- and third-order Møller-Plesset (MP2 and MP3) correlation energies E_c^{MP2} and E_c^{MP3}, and the exact and HF energies yield the correlation energy

$$E_{\mathrm{c}} = E_{\mathrm{exact}} - E_{\mathrm{HF}}. \tag{5}$$

III. ATOMS

A. Hydrogen-like ions

The electronic Hamiltonian of the 1D H-like ion with nucleus of charge Z at $x = 0$ is

$$\hat{H} = -\frac{1}{2}\frac{d^2}{dx^2} - \frac{Z}{|x|}, \tag{6}$$

and this has been studied in great detail (see [44, 51–53, 56, 57] and references therein), giving rise to much controversy over the nature of such a Hamiltonian and the eigenfunctions that it permits.

The heart of this argument lies in a difficulty that emerges from the unusually strong Coulomb singularity in 1D. This singularity becomes non-integrable in the limited dimensionality, which causes the Hamiltonian above to be unbounded and hence not self-adjoint. Such a Hamiltonian cannot provide the energy of the system and we must find an appropriate extension of it that does. Such extensions are equivalent to defining a set of boundary conditions for the eigenfunctions at the positions of the nuclei.

There are a family of possible extensions [65, 66] and it is not clear *a priori* which is the most appropriate. However, Oliveira and Verri [67, 68] have shown that, when restricting the system to a sequence of increasingly narrow 3D cylinders, only Dirichlet boundary conditions permit finite energies and thereby give rise to physically meaningful results. This also agrees with previous, similar studies [65, 78]. The eigenfunctions consistent with these boundary

conditions are

$$\psi_n^+(x) = xL_{n-1}^{(1)}(+2Zx/n)\exp(-Zx/n), \qquad x > 0, \tag{7}$$

$$\psi_n^-(x) = xL_{n-1}^{(1)}(-2Zx/n)\exp(+Zx/n), \qquad x < 0, \tag{8}$$

where $L_n^{(a)}$ is a Laguerre polynomial [77] and $n = 1, 2, 3, \ldots$. These eigenfunctions vanish at the nucleus, satisfying the boundary condition $\psi_n(0) = 0$.

It is tempting to combine these two sets of functions into families of even and odd parity. However, this is not admissible [57, 69] because the Dirichlet boundary conditions require that the nuclei be impenetrable to the electrons [79], as stated above.

Núñez-Yépez and coworkers [69] have provided the following justification for this impenetrability. Taking the hydrogen-like ion described by the Hamiltonian above and computing its quantum flux $j(x)$ at the nucleus, we find

$$j(0) = i\left(\psi_n \frac{d\psi_n^*}{dx} - \psi_n^* \frac{d\psi_n}{dx}\right)\Bigg|_{x=0} = 0 \tag{9}$$

where ψ_n is the electronic wavefunction and the boundary conditions imply $\psi_n(0) = 0$. It is clear from this that there is no passage of electrons in either direction across the nucleus. Instead there is total reflection of the electron and the nucleus is impenetrable. An immediate, but curious, consequence of this is that any odd-electron 1D atom has a non-vanishing dipole moment. The ground state of the 1D H atom, for example, has $\langle x \rangle = \pm 1.5$.

B. Helium-like ions

The electronic Hamiltonian of the 1D He-like ion is

$$\hat{H} = -\frac{1}{2}\left(\frac{\partial^2}{\partial x_1^2} + \frac{\partial^2}{\partial x_2^2}\right) - \frac{Z}{|x_1|} - \frac{Z}{|x_2|} + \frac{1}{|x_1 - x_2|} \tag{10}$$

and two families of electronic states can be considered:

- The one-sided $\mathrm{A}_{i,j}^{Z-2}$ family where both electrons are on the same side of the nucleus;
- The two-sided ${}_i\mathrm{A}_j^{Z-2}$ family where the electrons are on opposite sides of the nucleus.

Some of the properties of the first ten ions are gathered in Table I.

1. One-sided or two-sided?

Because of the constraints of movement in 1D, electrons shield one another very effectively and, as a result, the outer electron lies far from the nucleus in the $A_{1,2}^{Z-2}$ state. Because of this, the $A_{1,2}^{Z-2}$ state is significantly higher in energy than the ${}_1A_1^{Z-2}$ state. For example, the HF energies of $He_{1,2}$ and ${}_1He_1$ are -2.107356 and -3.242922, respectively.

In the hydride anion H^- ($Z = 1$), the nucleus cannot bind the second electron in the $H_{1,2}^-$ state and this species autoionizes. The corresponding state of the helium atom is bound but its ionization energy is only 0.1074. Whereas the minimum nuclear charge which can bind two electrons is $Z_{\rm crit} \approx 1.1$ in the $A_{1,2}^{Z-2}$ state, it is $Z_{\rm crit} \approx 0.65$ in the ${}_1A_1^{Z-2}$ state. In comparison, Baker *et al.* have reported [80] that the corresponding value in 3D is $Z_{\rm crit} \approx 0.91$.

In the ${}_1A_1^{Z-2}$ state, each electron is confined to one side of the nucleus, and is perfectly shielded from the other electron by the nucleus. As a result, the electron correlation energy $E_{\rm c}$ is entirely of the dispersion type and is much smaller than in 3D atoms. For example, $E_{\rm c}$ in ${}_1He_1$ is -3.022 while $E_{\rm c}$ in the ground state of 3D He is -42.024. It is interesting to note that, unlike the situation in 3D, the correlation energy of ${}_1H_1^-$ is slightly larger than in ${}_1He_1$ and approaches the large-Z limit from below.

Table I also shows that correlation energies $E_c^{\rm soft}$ arising from use of the softened Coulomb operator [23] are totally different from energies $E_{\rm c}$ from the unmodified operator. This qualitative change arises because the softened operator allows the electrons to share the same orbital.

2. Large-Z expansion

In the large-Z (i.e. high-density) limit, the exact and HF energies of the two-sided He-like ions can be expanded as a power series using Rayleigh-Schrödinger perturbation theory [81]

$$E_{\rm exact} = E^{(0)}\, Z^2 + E^{(1)}\, Z + E^{(2)} + \frac{E^{(3)}}{Z} + O(Z^{-2}), \tag{11}$$

$$E_{\rm HF} = E_{\rm HF}^{(0)}\, Z^2 + E_{\rm HF}^{(1)}\, Z + E_{\rm HF}^{(2)} + \frac{E_{\rm HF}^{(3)}}{Z} + O(Z^{-2}), \tag{12}$$

where

$$E^{(0)} = E^{(0)}_{\rm HF} = -1, \qquad E^{(1)} = E^{(1)}_{\rm HF} = 2/5. \tag{13}$$

For large Z, the limiting correlation energy is thus

$$E_{\rm c} = E^{(2)} - E^{(2)}_{\rm HF} + \frac{E^{(3)} - E^{(3)}_{\rm HF}}{Z} + O(Z^{-2}) = E^{(2)}_{\rm c} + \frac{E^{(3)}_{\rm c}}{Z} + O(Z^{-2}). \tag{14}$$

The second- and third-order exact energies

$$E^{(2)} = -0.045545, \qquad E^{(3)} = -0.000650, \tag{15}$$

can be found by Hylleraas' approach [82], while the second- and third-order HF energies

$$E^{(2)}_{\rm HF} = -0.042832, \qquad E^{(3)}_{\rm HF} = -0.000495, \tag{16}$$

can be found by Linderberg's method [83, 84]. We conclude, therefore, that

$$E_{\rm c} = -2.713 - \frac{0.155}{Z} + O(Z^{-2}). \tag{17}$$

The negative sign of $E^{(3)}_{\rm c}$ explains the reduction in the correlation energy as Z increases.

It is interesting to note that the 2D and 3D values of $E^{(2)}_{\rm c}$ are -220.133 and -46.663, respectively [81, 85, 86], which are much larger than the corresponding 1D values.

C. Periodic Table

We have computed the ground-state energies of the 1D atoms from Li to Ne at the HF, MP2 and MP3 levels. We have also computed these energies for their cations and anions. To compute the exact energy of Li and Be^+, we have used a Hylleraas-type wavefunction containing a large number of terms. The results are reported in Table II and the HF ground state of the first six atoms are represented in Fig. 2.

Where exact energies are available, it appears that the MP2 and MP3 calculations recover a large proportion of the exact correlation energy. Their performance appears to improve

rapidly as the atomic number grows and, for this reason, we consider the MP3 energies to be reliable benchmarks for the heavy atoms.

In view of the modest sizes of these atomic correlation energies, we conclude that it is likely that, for 1D systems, even the simple HF model is reasonably accurate and MP2 offers a very accurate theoretical model chemistry.

The accuracy of perturbative methods throughout Table II may be surprising given the small band gaps in some of the species, e.g. Li. Although a small gap is often an indicator of poor performance for perturbative corrections, the associated HOMO-LUMO excitations correspond to the movement of an electron from the outermost orbital on one side of the nucleus to the corresponding orbital on the other side, e.g. exciting from ${}_1\mathrm{Li}_{1,2}$ to ${}_{1,2}\mathrm{Li}_1$. However, such excitations are excluded from the perturbation sums because they involve the (physically forbidden) movement of an electron from one domain to another.

We have computed the ionization energy IE ($\mathrm{A} \longrightarrow \mathrm{A}^+ + \mathrm{e}^-$) and the electron affinity EA ($\mathrm{A} + \mathrm{e}^- \longrightarrow \mathrm{A}^-$) of each atom and these are summarised in Table III. Our HF calculations revealed that anions of even-Z atoms (viz. He^-, Be^-, C^-, O^- and Ne^-) autoionize. The IEs display a clear zig-zag pattern as the atomic number grows, reminiscent of the IEs in 3D. However, in 1D the period is very short, viz. two.

The odd-Z atoms have a non-zero dipole moment, which allows reactivity with other odd-Z atoms via dipole-dipole interactions. In contrast, the even-Z atoms have only a quadrupole and would be expected to be more electrostatically inert. The combination of the periodic trends in the IEs and the pattern of atomic reactivities allows us to construct a periodic table for 1D atoms (Fig. 3). The 1D atoms H, Li, B, N and F are the analogs of the 3D alkali metals (i.e. H, Li, Na, K and Rb) and the 1D atoms He, Be, C, O and Ne are the analogs of the 3D noble gases (i.e. He, Ne, Ar, Kr and Xe).

Like their 3D analogs [87–92], the 1D IEs drop as the nuclear charge increases. However, this behaviour is more dramatic in 1D than in 3D because the strong shielding in 1D causes the outermost electrons to be very weakly attracted to the nucleus. This effect is so powerful that the third 1D noble gas (C) has an IE (4.733 eV) which is lower than the IE (5.139 eV) of the third 3D alkali metal (Na).

1D EAs also behave similarly to their 3D counterparts, decreasing as the nuclear charge increases. Because one side of the nucleus is completely unshielded, the EA of 1D H (3.961 eV) is far larger than that of 3D H (0.754 eV). However, like the 1D IEs, shielding effects

lead to a rapid reduction in EA as the nuclear charge increases. As a result, the fifth 1D alkali metal (F) has an EA (0.160 eV) which is considerably smaller than the EA (0.486 eV) of the fifth 3D alkali metal (Rb).

We have also computed $\sqrt{\langle x^2 \rangle}$ as a measure of atomic radius and compared these to the calculated values of Clementi *et al.* [93, 94] for 3D atoms. Whereas a 3D alkali metal atom is much larger than the noble gas atom of the same period, the 1D alkali metal atoms are only slightly larger than their noble gas counterparts.

IV. MOLECULES

A. One-electron diatomics

The electronic Hamiltonian of a one-electron diatomic $AB^{Z_A+Z_B-1}$ composed of two nuclei A and B of charges Z_A and Z_B located at $x = -R/2$ and $x = +R/2$ is

$$\hat{H} = -\frac{1}{2}\frac{d^2}{dx^2} - \frac{Z_A}{|x + R/2|} - \frac{Z_B}{|x - R/2|}. \tag{18}$$

For these systems, three families of states are of interest:

- The ${}_iAB^{Z_A+Z_B-1}$ and $AB_i^{Z_A+Z_B-1}$ families where the electron is outside the nuclei [95];
- The $A_iB^{Z_A+Z_B-1}$ family where the electron is between the two nuclei.

Some of the properties of three such systems are reported in the upper half of Table IV.

1. H_2^+

The simplest of all molecules is the homonuclear diatomic H_2^+, in which $Z_A = Z_B = 1$. In 3D, this molecule was first studied by Burrau who pointed out that the Schrödinger equation is separable in confocal elliptic coordinates [96]. In 1928, Linus Pauling published a review summarizing the work of Burrau and many other researchers [97, 98]. In Appendix A, we report some exact wavefunctions for H_1H^+ in 1D.

The near-exact potential energy curves of the H_1H^+ and HH_1^+ states are shown in Fig. 4. Beyond $R = 1.5$, the H_1H^+ state is lower in energy than the HH_1^+ state. However, when the bond is compressed, the kinetic energy of the trapped electron becomes so large that the

H_1H^+ state rises above the HH_1^+ state. The bond dissociation energy (0.3307 E_h) of H_1H^+ is large and its equilibrium bond length ($R_{eq} = 2.581$ bohr) is long. Both values are much larger than the corresponding 3D values (0.1026 E_h and 1.997 bohr) [99]. Note that the electrostatic forces within the H_1H^+ state are attractive due to a favorable charge-dipole interaction, while those of the HH_1^+ state are repulsive because of a similar, but unfavorable, interaction. Using this simple argument, one can predict that the H_1H^+ and HH_1^+ potential energy curves behave as $-\mu_H/R^2$ and $+\mu_H/R^2$ for large R, where $\mu_H = 3/2$. This charge-dipole model is qualitatively correct for $R \gtrsim 10$ for H_1H^+ and $R \gtrsim 5$ for HH_1^+.

2. *HeH^{2+} and He_2^{3+}*

The Hamiltonians of HeH^{2+} and He_2^{3+} are given by (18) for $Z_A = 1$ and $Z_B = 2$, and $Z_A = Z_B = 2$, respectively. As in H_2^+, we find that He_1He^{3+} is more stable than $HeHe_1^{3+}$, and He_1H^{2+} is more stable than HeH_1^{2+} and $_1HeH^{2+}$, except at short bond lengths.

In 3D, the molecules HeH^{2+} and He_2^{3+} are unstable except in strong magnetic fields [100]. However, as Fig. 5 shows, He_1H^{2+} and He_1He^{3+} are metastable species in 1D with equilibrium bond lengths of $R_{eq} = 2.182$ and 1.793, and transition structure bond lengths of $R_{ts} = 3.296$ and 4.630, respectively. Although these species are thermodynamically unstable with respect to $He^+ + H^+$ and $He^+ + He^{2+}$, they are protected from dissociation by barriers of 0.0209 and 0.2924, respectively. For large R, their dissociation curves behave as $1/R - \mu_{He^+}/R^2$ and $2/R - 2\mu_{He^+}/R^2$, respectively, where $\mu_{He^+} = 3/4$.

All the heavier one-electron diatomics have purely repulsive dissociation curves.

3. *Chemical bonding in one-electron diatomics*

Fig. 6 shows the electronic density $\rho(x)$ for H_1H^+ and He_1H^{2+} at their equilibrium bond lengths. Whereas the electron density in a typical 3D bond is greatest at the nuclei and reaches a minimum near the middle of the bond [98], the electron density in these 1D bonds vanishes at the nuclei and achieves a maximum in the middle of the bond. The bond in He_1H^{2+} is polarized towards the nucleus with the largest charge.

4. Harmonic vibrations

We have computed the harmonic vibrational frequencies of H_1H^+, He_1H^{2+} and He_1He^{3+} at their equilibrium bond lengths and these are shown in Table IV. The second derivative of the energy was obtained numerically using the three-point central difference formula and a stepsize of 10^{-2} bohr. The frequency of the 1D H_1H^+ ion (2470 cm^{-1}) is similar to that of the 3D ion (2321 cm^{-1}) [101] but this result is probably accidental. Although the barrier in He_1H^{2+} is small and its harmonic frequency relatively high (3553 cm^{-1}), the ion probably supports a vibrational state: the zero-point vibrational energy is only half the barrier height.

B. Two-electron diatomics

The Hamiltonian of a two-electron diatomic $AB^{Z_A+Z_B-2}$ composed of two nuclei A and B of charges Z_A and Z_B located at $x = -R/2$ and $x = +R/2$ is

$$\hat{H} = -\frac{1}{2}\left(\frac{\partial^2}{\partial x_1^2} + \frac{\partial^2}{\partial x_2^2}\right) - \frac{Z_A}{\left|x_1 + \frac{R}{2}\right|} - \frac{Z_A}{\left|x_2 + \frac{R}{2}\right|} - \frac{Z_B}{\left|x_1 - \frac{R}{2}\right|} - \frac{Z_B}{\left|x_2 - \frac{R}{2}\right|} + \frac{1}{|x_1 - x_2|}. \quad (19)$$

These systems possess six families of states:

- The $A_{i,j}B^{Z_A+Z_B-2}$ family;
- The ${}_iAB_j^{Z_A+Z_B-2}$ family;
- The ${}_iA_jB^{Z_A+Z_B-2}$ and $A_iB_j^{Z_A+Z_B-2}$ families [95];
- The ${}_{i,j}AB^{Z_A+Z_B-2}$ and $AB_{i,j}^{Z_A+Z_B-2}$ families [95];

Some of the properties of four such systems are reported in the lower half of Table IV.

1. H_2

The simplest two-electron diatomic is H_2 where $Z_A = Z_B = 1$. The 3D version of this molecule has been widely studied since the first accurate calculation of James and Coolidge [75] in 1933. The ground state in each family has been calculated using Hylleraas-type calculations and is represented in Fig. 7. We note that the HF and Hylleraas curves are almost indistinguishable due to the small correlation energy in these systems (see Table IV).

As expected, $HH_{1,2}$ is high in energy due to shielding by the inner electron (see discussion on the He-like ions in Sec. III B), and dissociates into $H^+ + H^-_{1,2}$. The three other states dissociate into a pair of H atoms. As in H_2^+, the $_1HH_1$ state is the most stable at small bond lengths, but is higher in energy than H_1H_1 when $R > 1.5$ bohr. The H_1H_1 state is bound with an equilibrium bond length of 2.639 bohr and a dissociation energy of 0.1859 E_h. In comparison, the bond length of the 3D H_2 molecule is close to 1.4 bohr and has a similar dissociation energy (0.1745 E_h) [102]. The harmonic vibrational frequency of H_1H_1 (2389 cm^{-1}) is significantly lower than the 3D value (4401 cm^{-1}) [101]. The equilibrium bond lengths and vibrational frequencies of H_1H^+ and H_1H_1 are similar because of the efficient shielding in 1D. Finally, we note that H_1H_1 has a non-zero dipole moment and the two H_1 fragments experience an attractive dipole-dipole interaction.

For those who are familiar with the traditional covalent two-electron bond in 3D chemistry, the instability of $H_{1,2}H$ is probably surprising. However, this state is destabilized by two important effects: (a) the high kinetic energy of the electrons when trapped between nuclei (see discussion on H_2^+ in Sec. IV A) and (b) the 1D exclusion principle, which mandates that the second electron occupy a higher-energy orbital than the first. For these reasons, 1D molecules are usually held together by one-electron bonds (sometimes called hemi-bonds).

Bonding in H_2^+, which is held together by the $H^+ + H$ charge-dipole interaction, is roughly twice as strong as the bonding in H_2, which is bound by a much weaker $H + H$ dipole-dipole interaction. In contrast, in 3D, the H_2 bond is roughly twice as strong as that in H_2^+.

We expect that two-electron (or more) bonds exist in neutral species such as $_1Li_{1,2}H_1$ because of favorable dipole-dipole interactions. However, such species are bound *despite* the two-electron bond, rather than because of it, and are probably very weakly bound. We will investigate this further in a forthcoming paper [76].

2. HeH^+ and He_2^{2+}

The Hamiltonian for HeH^+ and He_2^{2+} are given by (19) for $Z_A = 1$ and $Z_B = 2$, and $Z_A = Z_B = 2$, respectively. Like He_1He^{3+}, $He_1He_1^{2+}$ is metastable with a large energy barrier of 0.3051 E_h and a late transition structure with $R_{ts}/R_{eq} \approx 2.5$. In 3D, the He_2^{2+} dication is also metastable but with an earlier transition structure ($R_{ts}/R_{eq} \approx 1.5$) [103–107].

Like the 3D HeH^+ molecule [108], the 1D $_1He_1H^+$ and $He_1H_1^+$ ions are bound. The

dissociation of ${}_1\mathrm{He}_1\mathrm{H}^+$ into ${}_1\mathrm{He}_1 + \mathrm{H}^+$ requires 0.1981 E_h and is much more endothermic than the dissociation of $\mathrm{He}_1\mathrm{H}_1^+$ into $\mathrm{He}_1^+ + \mathrm{H}_1$, which requires only 0.0174 E_h. Surprisingly, however, they have similar bond lengths and harmonic frequencies.

3. Chemical bonding in two-electron diatomics

Fig. 8 shows the electronic densities $\rho(x)$ in $\mathrm{H}_1\mathrm{H}_1$, $\mathrm{H}_1\mathrm{He}_1^+$, $\mathrm{He}_1\mathrm{H}_1^+$ and $\mathrm{He}_1\mathrm{He}_1^{2+}$ at their respective equilibrium bond lengths. The bonds in $\mathrm{H}_1\mathrm{H}_1$ and $\mathrm{He}_1\mathrm{He}_1^{2+}$ are polar because of the repulsion by the external electron. In $\mathrm{He}_1\mathrm{H}_1^+$, the bond is highly polar because the repulsion by the external electron and the attraction of the He nucleus push in the same direction. In $\mathrm{H}_1\mathrm{He}_1^+$, the bond is polarized in the opposite direction because the repulsion by the external electron is dominated by the attraction of the He nucleus.

4. Correlation effects

Table IV reports the MP2, MP3 and exact correlation energies at the equilibrium geometries of $\mathrm{H}_1\mathrm{H}_1$, ${}_1\mathrm{He}_1\mathrm{H}^+$, $\mathrm{He}_1\mathrm{H}_1^+$ and $\mathrm{He}_1\mathrm{He}_1^{2+}$. All these values are small compared to their 3D analogs because correlation energy in these 1D systems is entirely due to dispersion. As a result, correlation effects are pleasingly small and, for example, the HF bond length in $\mathrm{H}_1\mathrm{H}_1$ differs from the exact value by only 0.003 bohr. This re-emphasizes that the HF approximation is probably significantly more accurate in 1D than in 3D.

The range of E_c values (-2.434 in $\mathrm{H}_1\mathrm{He}_1^+$, -1.771 in $\mathrm{He}_1\mathrm{He}_1^{2+}$, -1.377 in $\mathrm{H}_1\mathrm{H}_1$, -0.671 in $\mathrm{He}_1\mathrm{H}_1^+$) can be rationalized by comparing the distance between the two electrons in each system (see Fig. 8): shorter distances yield larger correlation energies.

For the diatomics in Table IV, HF theory is again found to be accurate and the MPn series appears to converge rapidly towards the exact correlation energies. As in the atomic cases (see Sec. III C), MP2 and MP3 calculations recover a large fraction of the exact correlation energy.

C. Chemistry of H_3^+

The 3D H_3^+ ion was discovered by Thomson [109] in 1911 and plays a central role in interstellar chemistry [110–112]. In astrochemistry, the main pathway for its production is

$$H_2^+ + H_2 \longrightarrow H_3^+ + H \tag{20}$$

and this reaction is highly exothermic ($\Delta U = -0.0639\ E_h$) [112]. In 3D, the ion has a triangular structure [113] as first demonstrated by Coulson [114]. (See Ref. 112 for an interesting historical discussion on H_3^+.) The proton affinity of H_2

$$H_2 + H^+ \longrightarrow H_3^+ \tag{21}$$

is also strongly exothermic ($\Delta U = -0.1613\ E_h$) [115].

In this Section, we study the 1D analogs of these two reactions, viz.

$$H_1H^+ + {}_1H_1H \longrightarrow H_1H_1H^+ + {}_1H \tag{22}$$

$$H_1H_1 + H^+ \longrightarrow H_1H_1H^+ \tag{23}$$

In 1D, the equilibrium structure of $H_1H_1H^+$ has $D_{\infty h}$ symmetry, a bond length of 2.664 bohr, and an energy of $-1.570720\ E_h$ (see Table IV). The correlation energy at this bond length is only 0.900 mE_h. Our calculations predict that reactions (22) and (23) are both exothermic ($\Delta U = -0.0541$ and $-0.3848\ E_h$, respectively) and that reaction (23) is barrierless. It is interesting that the exothermicities of reactions (20) and (22) are close, and that the proton affinities (reactions (21) and (23)) are also broadly similar.

D. Hydrogen nanowire

Despite the fact that equi-spaced infinite H chain in 3D suffers from a Peierls instability [116], this system has attracted considerable interest due to its strong correlation character and metal-insulator transition [117–121]. We have therefore used periodic HF calculations [122, 123] to compute the energy per atom of an infinite chain of equi-spaced 1D H atoms separated by a distance R. Motivated by our results for 1D H_2^+, H_2 and H_3^+, we have studied

the state in which one electron is trapped between each pair of nuclei, i.e. $\cdots H_1H_1H_1H_1\cdots$.

We have expanded the HF orbital in the unit cell ($x \in [-R/2, R/2]$) as a linear combination of K even polynomials (3). We find that, near the minimum-energy structure, $K = 4$ suffices to achieve convergence of the HF energy to within one microhartree and the resulting bond length is $R_{\rm eq} = 2.795$, which is slightly longer than the values in H_2^+, H_2 and H_3^+. The corresponding energy is -0.710457 which yields a binding energy of 0.2105 per bond. In comparison, the binding energy in H_2 is roughly 80% of this value. This explains the particular stability of the equally-spaced H_∞ chain in 1D.

V. CONCLUDING REMARKS

We have studied the electronic structure of 1D chemical systems in which all nuclei and electrons are constrained to remain on a line. We have used the full Coulomb operator and our numerical results are strikingly different from those of previous studies [23, 24] in which a softened operator was used. We have explored atoms with up to 10 electrons, one- and two-electron diatomics, the chemistry of H_3^+ and an infinite chain of H atoms.

We find that, whereas atoms with odd numbers of electrons have non-vanishing dipole moments and are reactive, atoms with even numbers of electrons have zero dipole moments and are inert. Based on these results, we have concluded that the 1D version of the periodic table has only two groups: alkali metals and noble gases.

Our study of one- and two-electron diatomics has revealed that atoms in 1D are bound together by strong one-electron bonds. The Coulombic forces within such bonds can be accurately modelled by simple classical electrostatics, primarily as charge-dipole and dipole-dipole interactions. This leads to a variety of unexpected results, such as the discovery that the bond in H_2^+ is much stronger than the bond in H_2.

ACKNOWLEDGMENTS

We thank Giuseppe Barca for several illuminating discussions about impenetrability in 1D systems. P.F.L. and P.M.W.G. thank the NCI National Facility for generous grants of supercomputer time. P.M.W.G. thanks the Australian Research Council for funding (Grants No. DP120104740 and DP140104071). P.F.L. thanks the Australian Research Council for a

Discovery Early Career Researcher Award (Grant No. DE130101441) and a Discovery Project grant (DP140104071). C.J.B. is grateful for an Australian Postgraduate Award.

Appendix A: Some exact wavefunctions for H_2^+

The Schrödinger equation of a one-electron homonuclear diatomic molecule A_2^{Z-1} of nuclear charge Z in its state A_1A^{Z-1} is

$$-\frac{1}{2}\frac{d^2\psi(x)}{dx^2} - \left(\frac{Z}{R/2+x} + \frac{Z}{R/2-x}\right)\psi(x) = E\,\psi(x). \tag{A1}$$

The equation can be solved for $E = 0$, yielding

$$\psi_n(x) = (1-z^2)\begin{cases} x\,F\left(-\frac{n-1}{2}, \frac{n+4}{2}, 2, 1-z^2\right), & n \text{ odd}, \\ F\left(-\frac{n}{2}, \frac{n+3}{2}, 2, 1-z^2\right), & n \text{ even}, \end{cases} \tag{A2}$$

where $F(a,b,c,x)$ is the Gauss hypergeometric function [77], $z = 2x/R$ and

$$R = \frac{(n+1)(n+2)}{2Z}. \tag{A3}$$

For example, H_2^+ with bond length $R = 1$ has the wavefunction $\psi_0(x) = (1-2x)(1+2x)$.

[1] R. Saito, G. Dresselhaus, and M. S. Dresselhaus, *Properties of Carbon Nanotubes* (Imperial College Press, London, 1998).

[2] R. Egger and A. O. Gogolin, Eur. Phys. J. B **3**, 281 (1998).

[3] M. Bockrath, D. H. Cobden, J. Lu, A. G. Rinzler, R. E. Smalley, L. Balents, and P. L. McEuen, Nature **397**, 598 (1999).

[4] H. Ishii, H. Kataura, H. Shiozawa, H. Yoshioka, H. Otsubo, Y. Takayama, T. Miyahara, S. Suzuki, Y. Achiba, M. Nakatake, T. Narimura, M. Higashiguchi, K. Shimada, H. Namatame, and M. Taniguchi, Nature **426**, 540 (2003).

[5] M. Shiraishi and M. Ata, Sol. State Commun. **127**, 215 (2003).

[6] A. Schwartz, M. Dressel, G. Grüner, V. Vescoli, L. Degiorgi, and T. Giamarchi, Phys. Rev. B **58**, 1261 (1998).

[7] V. Vescoli, F. Zwick, W. Henderson, L. Degiorgi, M. Grioni, G. Gruner, and L. K. Montgomery, Eur. Phys. J. B **13**, 503 (2000).

[8] T. Lorenz, M. Hofmann, M. Grüninger, A. Freimuth, G. S. Uhrig, M. Dumm, and M. Dressel, Nature **418**, 614 (2002).

[9] M. Dressel, K. Petukhov, B. Salameh, P. Zornoza, and T. Giamarchi, Phys. Rev. B **71**, 075104 (2005).

[10] T. Ito, A. Chainani, T. Haruna, K. Kanai, T. Yokoya, S. Shin, and R. Kato, Phys. Rev. Lett. **95**, 246402 (2005).

[11] Z. Hu, M. Knupfer, M. Kielwein, U. K. Roẗler, M. S. Golden, J. Fink, F. M. F. de Groot, T. Ito, K. Oka, and G. Kaindl, Eur. Phys. J. B **26**, 449 (2002).

[12] F. P. Milliken, C. P. Umbach, and R. A. Webb, Sol. State Commun. **97**, 309 (1996).

[13] S. S. Mandal and J. K. Jain, Sol. State Commun. **118**, 503 (2001).

[14] A. M. Chang, Rev. Mod. Phys. **75**, 1449 (2003).

[15] A. R. Goni̇, A. Pinczuk, J. S. Weiner, J. M. Calleja, B. S. Dennis, L. N. Pfeiffer, and K. W. West, Phys. Rev. Lett. **67**, 3298 (1991).

[16] O. M. Auslaender, A. Yacoby, R. dePicciotto, K. W. Baldwin, L. N. Pfeiffer, and K. W. West, Phys. Rev. Lett. **84**, 1764 (2000).

[17] S. V. Zaitsev-Zotov, Y. A. Kumzerov, Y. A. Firsov, and P. Monceau, J. Phys.: Condens. Matter **12**, L303 (2000).

[18] F. Liu, M. Bao, K. L. Wang, C. Li, B. Lei, and C. Zhou, Appl. Phys. Lett. **86**, 213101 (2005).

[19] H. Steinberg, O. M. Auslaender, A. Yacoby, J. Qian, G. A. Fiete, Y. Tserkovnyak, B. I. Halperin, K. W. Baldwin, L. N. Pfeiffer, and K. W. West, Phys. Rev. B **73**, 113307 (2006).

[20] H. Monien, M. Linn, and N. Elstner, Phys. Rev. A **58**, R3395 (1998).

[21] A. Recati, P. O. Fedichev, W. Zwerger, and P. Zoller, J. Opt. B: Quantum Semiclass. Opt. **5**, S55 (2003).

[22] H. Moritz, T. Stoferle, K. Guenter, M. Kohl, and T. Esslinger, Phys. Rev. Lett. **94**, 210401 (2005).

[23] L. O. Wagner, E. Stoudenmire, K. Burke, and S. R. White, Phys. Chem. Chem. Phys. **14**, 8581 (2012).

[24] E. M. Stoudenmire, L. O. Wagner, S. R. White, and K. Burke, Phys. Rev. Lett. **109**, 056402 (2012).

[25] R. G. Parr and W. Yang, *Density-functional theory of atoms and molecules* (Oxford, Clarendon Press, 1989).

[26] D. J. Doren and D. R. Herschbach, Chem. Phys. Lett. **118**, 115 (1985).

[27] J. G. Loeser and D. R. Herschbach, J. Chem. Phys. **84**, 3882 (1986).

[28] J. G. Loeser and D. R. Herschbach, J. Chem. Phys. **84**, 3893 (1986).

[29] C. M. Rosenthal, J. Chem. Phys. **55**, 2474 (1971).

[30] L. L. Foldy, Am. J. Phys. **44**, 1192 (1976).

[31] L. L. Foldy, Am. J. Phys. **45**, 1230 (1977).

[32] Y. Nogami, M. Vallieres, and W. van Dijk, Am. J. Phys. **44**, 886 (1976).

[33] J. G. Loeser and D. R. Herschbach, J. Phys. Chem. **89**, 3444 (1985).

[34] D. R. Herschbach, J. Chem. Phys. **84**, 838 (1986).

[35] D. J. Doren and D. R. Herschbach, J. Chem. Phys. **87**, 433 (1987).

[36] J. G. Loeser and D. R. Herschbach, J. Chem. Phys. **86**, 3512 (1987).

[37] G. E. Astrakharchik and M. D. Girardeau, Phys. Rev. B **83**, 153303 (2011).

[38] R. M. Lee and N. D. Drummond, Phys. Rev. B **83**, 245114 (2011).

[39] P. F. Loos and P. M. W. Gill, Phys. Rev. Lett. **108**, 083002 (2012).

[40] P. F. Loos, J. Chem. Phys. **138**, 064108 (2013).

[41] P. F. Loos and P. M. W. Gill, J. Chem. Phys. **138**, 164124 (2013).

[42] P. F. Loos, C. J. Ball, and P. M. W. Gill, J. Chem. Phys. **140**, 18A524 (2014).

[43] P. F. Loos, Phys. Rev. A **89**, 052523 (2014).

[44] R. Loudon, Am. J. Phys. **27**, 649 (1959).

[45] K. Burnett, V. C. Reed, and P. L. Knight, J. Phys. B: At. Mol. Opt. Phys. **26**, 561 (1993).

[46] M. Mayle, B. Hezel, I. Lesanovsky, and P. Schmelcher, Phys. Rev. Lett. **99**, 113004 (2007).

[47] M. M. Nieto, Phys. Rev. A **61**, 034901 (2000).

[48] S. H. Patil, Phys. Rev. A **64**, 064902 (2001).

[49] P. M. Platzman and M. I. Dykman, Science , 1967 (1999).

[50] M. I. Dykman, P. M. Platzman, and P. Seddighrad, Phys. Rev. B **67**, 155402 (2003).

[51] M. Andrews, Am. J. Phys. **44**, 1064 (1976).

[52] H. N. Núñez-Yépez, C. A. Varga, and A. L. Salas-Brito, Eur. J. Phys. **8** (1987).

[53] L. J. Boya, M. Kmiecik, and A. Bohm, Phys. Rev. A **37**, 3567 (1988).

[54] V. S. Mineev, Theor. Math. Phys. **140**, 1157 (2004).

[55] C. R. de Oliveira and A. A. Verri, Ann. Phys. **324**, 251 (2009).

[56] G. Abramovici and Y. Avishai, J. Phys. A **42**, 285302 (2009).

[57] H. N. Núñez-Yépez, A. L. Salas-Brito, and D. A. Solis, Phys. Rev. A **83**, 064101 (2011).

[58] T. D. Imbo and U. P. Sukhatme, Phys. Rev. Lett. **54**, 2184 (1985).

[59] H. N. Núñez-Yépez and A. L. S. Brito, Eur. J. Phys. **8**, 307 (1987).

[60] H. N. Núñez-Yépez, C. A. Varga, and A. L. Salas-Brito, Phys. Rev. A **39**, 4306 (1989).

[61] M. Moshinsky, J. Phys. A **26**, 2445 (1993).

[62] R. G. Newton, J. Phys. A **27**, 4717 (1994).

[63] D. Xianxi, J. Dai, and J. Dai, Phys. Rev. A **55**, 2617 (1997).

[64] K. Connolly and D. J. Griffiths, Am. J. Phys. **75**, 524 (2007).

[65] W. Fischer, H. Leschke, and P. Müller, J. Math. Phys. **36**, 2313 (1995).

[66] C. R. de Oliveira and A. A. Verri, Ann. Phys. **324**, 251 (2009).

[67] C. R. de Oliveira, Phys. Lett. A **374**, 2805 (2010).

[68] C. R. de Oliveira and A. A. Verri, J. Math. Phys. **53**, 052104 (2012).

[69] H. N. Núñez-Yépez, A. L. Salas-Brito, and D. A. Solis, Phys. Rev. A **89**, 049908(E) (2014).

[70] In a previous study of a different 1D system [39] we explored the nodal structure of the wavefunction. We discovered that the ground state has the minimal number of nodes. The node present when electrons touch is required in 1D systems however, due to the unusually strong singularity of the Coulomb operator. As a result this set of nodes is a complete description of the nodes found in the ground state wavefunction. We also showed that excited states contain further nodes in their wavefunctions, such states have not been explored here however.

[71] L. Mitas, Phys. Rev. Lett. **96**, 240402 (2006).

[72] A. Szabo and N. S. Ostlund, *Modern quantum chemistry* (McGraw-Hill, New York, 1989).

[73] E. A. Hylleraas, Z. Phys. **54**, 347 (1929).

[74] E. A. Hylleraas, Adv. Quantum Chem. **1**, 1 (1964).

[75] H. M. James and A. S. Coolidge, J. Chem. Phys. **1**, 825 (1933).

[76] C. J. Ball, P. F. Loos, and P. M. W. Gill, , in preparation.

[77] F. W. J. Olver, D. W. Lozier, R. F. Boisvert, and C. W. Clark, eds., *NIST handbook of mathematical functions* (Cambridge University Press, New York, 2010).

[78] F. Gesztesy, J. Phys. A: Math. Gen. **13**, 867 (1980).

[79] It is important to note that electrons are also impenetrable to one another. This follows as a result of the node required in the wavefunction when electrons coalesce [71]. If we compute the quantum flux across the position of one of the electrons we find it to be zero, implying that there can be no particle flow from the left of the electron to the right. This argument is analogous, though complicated by the electrons not being fixed, to that presented in Sec. III to show that nuclei are impenetrable. Alternatively, one may view the wavefunction node as an extension of the Dirichlet boundary conditions to the electrons.

[80] J. D. Baker, D. E. Freund, R. Nyden Hill, and J. D. Morgan III, Phys. Rev. A **41**, 1247 (1990).

[81] P. F. Loos and P. M. W. Gill, J. Chem. Phys. **131**, 241101 (2009).

[82] E. A. Hylleraas, Z. Phys. **65**, 209 (1930).

[83] J. Linderberg and H. Shull, J. Mol. Spectrosc. **5**, 1 (1960).

[84] J. Linderberg, Phys. Rev. **121**, 816 (1961).

[85] P. F. Loos and P. M. W. Gill, Phys. Rev. Lett. **105**, 113001 (2010).

[86] P. F. Loos and P. M. W. Gill, Chem. Phys. Lett. **500**, 1 (2010).

[87] K. R. Lykke, K. K. Murray, and W. C. Lineberger, Phys. Rev. A **43**, 6104 (1991).

[88] G. Haeffler, G. Hanstorp, I. K. A. E. Klinkmüller, U. Ljungblad, and D. J. Pegg, Phys. Rev. A **53**, 4127 (1996).

[89] H. Hotop and W. C. Lineberger, J. Phys. Chem. Ref. Data **14**, 731 (1985).

[90] K. T. Andersson, J. Sandstrom, I. Y. Kiyan, D. Hanstorp, and D. J. Pegg, Phys. Rev. A **62**, 022503 (2000).

[91] P. Frey, F. Breyer, and H. Hotop, J. Phys. B **11**, L589 (1978).

[92] D. R. Lide, ed., "CRC handbook of chemistry and physics," (CRC Press, Boca Raton, Florida, 2003) Chap. 10: Atomic, Molecular, and Optical Physics; Ionization Potentials of Atoms and Atomic Ions, 84th ed.

[93] E. Clementi and D. L. Raimond, J. Chem. Phys. **38**, 2686 (1963).

[94] E. Clementi, D. L. Raimond, and W. P. Reinhardt, J. Chem. Phys. **47** (1967).

[95] In the homonuclear case, i.e. $Z_{\mathrm{A}} = Z_{\mathrm{B}}$, these two families are equivalent.

[96] O. Burrau, Naturwissenschaften **15**, 16 (1927).

[97] L. Pauling, Chem. Rev. **5**, 173 (1928).

[98] L. Pauling and E. B. Wilson, *Introduction to Quantum Mechnics with Applications to Chemistry* (Dover, 1985).

[99] T. C. Scott, M. Aubert-Frecon, and J. Grotendorst, Chem. Phys. **324**, 323 (2006).

[100] A. V. Turbiner, J. C. Lopez-Vieyra, and N. L. Guevara, Phys. Rev. A **81**, 042503 (2010).

[101] K. P. Huber and G. Herzberg, *Molecular Spectra and Molecular Structure: IV. Constants of diatomic molecules* (van Nostrand Reinhold Company, 1979).

[102] W. Kolos and L. Wolniewicz, J. Chem. Phys. **49**, 404 (1968).

[103] L. Pauling, J. Chem. Phys. **1**, 56 (1933).

[104] M. Guilhaus, A. Brenton, J. Beynon, M. Rabrenovic, and P. R. Schleyer, J. Phys. B **17**, L605 (1984).

[105] P. M. W. Gill and L. Radom, Chem. Phys. Lett. **136**, 294 (1987).

[106] P. M. W. Gill and L. Radom, J. Am. Chem. Soc. **110**, 5311 (1988).

[107] P. M. W. Gill and L. Radom, Chem. Phys. Lett. **147**, 213 (1988).

[108] L. Wolniewicz, J. Chem. Phys. **43**, 1087 (1965).

[109] J. J. Thomson, Philos. Mag. **21**, 225 (1911).

[110] E. Herbst, Phil. Trans. R. Soc. A **358**, 2523 (2000).

[111] T. Oka, Proc. Nat. Am. Soc. **103**, 12235 (2006).

[112] T. Oka, Chem. Rev. **113**, 8738 (2013).

[113] F. Mentch and J. B. Anderson, J. Chem. Phys. **80**, 2675 (1984).

[114] C. A. Coulson, Proc. Cam. Philos. Soc. **31**, 244 (1935).

[115] G. D. Carney and R. N. Porter, J. Chem. Phys. **65**, 3547 (1976).

[116] M. Kertesz, J. Koller, and A. Azman, Theoret. Chim. Acta **41**, 89 (1976).

[117] J. Hachmann, W. Cardoen, and G. K. L. Chan, J. Chem. Phys. **125**, 144101 (2006).

[118] T. Tsuchimochi and G. E. Scuseria, J. Chem. Phys. **131**, 121102 (2009).

[119] A. V. Sinitskiy, L. Greenman, and D. A. Mazziotti, J. Chem. Phys. **133**, 014104 (2010).

[120] L. Stella, C. Attaccalite, S. Sorella, and A. Rubio, Phys. Rev. B **84**, 245117 (2011).

[121] D. Zgid and G. K. L. Chan, J. Chem. Phys. **134**, 094115 (2011).

[122] V. R. Saunders, Faraday Symp. Chem. Soc. **19**, 79 (1984).

[123] V. R. Saunders, C. Freyria-Fava, R. Dovesi, and C. Roetti, Comput. Phys. Commun. **84**, 156 (1994).

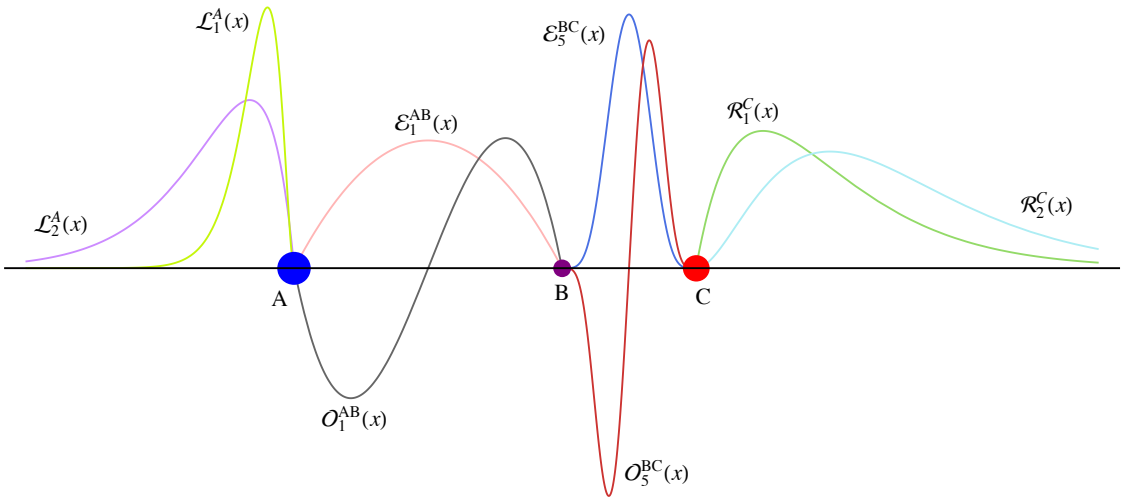

FIG. 1. Orbital basis functions in a triatomic molecule ABC

TABLE I. Total energies (in E_h), correlation energies (in mE_h), HOMO-LUMO gaps (in E_h) and radii (in a.u.) of the 1D helium-like ions

	Total energy		Correlation energy				HF property	
Ion	$-E_{\text{exact}}$	$-E_{\text{HF}}$	$-E_c^{\text{MP2}}$	$-E_c^{\text{MP3}}$	$-E_{\text{c}}$	$-E_c^{\text{soft}}$	Gap	$\sqrt{\langle x^2 \rangle}$
${}_1\text{H}_1^-$	0.646 584	0.643 050	1.713	2.530	3.534	39	0.170	2.296
${}_1\text{He}_1$	3.245 944	3.242 922	2.063	2.688	3.022	14	1.265	0.985
${}_1\text{Li}_1^+$	7.845 792	7.842 889	2.235	2.733	2.903	8	3.200	0.628
${}_1\text{Be}_1^{2+}$	14.445 725	14.442 873	2.335	2.747	2.851	6	5.874	0.460
${}_1\text{B}_1^{3+}$	23.045 686	23.042 864	2.401	2.751	2.822		9.294	0.364
${}_1\text{C}_1^{4+}$	33.645 661	33.642 859	2.447	2.752	2.802		13.463	0.301
${}_1\text{N}_1^{5+}$	46.245 644	46.242 855	2.481	2.751	2.789		18.382	0.256
${}_1\text{O}_1^{6+}$	60.845 631	60.842 852	2.508	2.749	2.779		24.050	0.223
${}_1\text{F}_1^{7+}$	77.445 621	77.442 849	2.529	2.748	2.772		30.468	0.198
${}_1\text{Ne}_1^{8+}$	96.045 613	96.042 847	2.546	2.746	2.766		37.635	0.177

TABLE II. Total energies (in E_h), correlation energies (in mE_h), HOMO-LUMO gaps (in E_h), dipole moments $\langle x \rangle$ and radii $\sqrt{\langle x^2 \rangle}$ (in a.u.) of 1D atoms and ions

	Energy		Correlation energy			HF property		
Ion	$-E_{\text{exact}}$	$-E_{\text{HF}}$	$-E_c^{\text{MP2}}$	$-E_c^{\text{MP3}}$	$-E_c$	Gap	$\langle x \rangle$	$\sqrt{\langle x^2 \rangle}$
H^+	0	0	0	0	0	—	0	0
H_1	0.500 000	0.500 000	0	0	0	0.373	1.500	1.732
${}_1H_1^-$	0.646 584	0.643 050	1.715	2.530	3.534	0.168	0	2.296
He_1^+	2.000 000	2.000 000	0	0	0	0.776	0.750	0.866
${}_1He_1$	3.245 944	3.242 922	2.063	2.688	3.022	1.264	0	0.985
${}_1He_{1,2}^-$			Autoionizes					
${}_1Li_1^+$	7.845 792	7.842 889	2.235	2.733	2.903	3.200	0	0.628
${}_1Li_{1,2}$	8.011 9	8.007 756	3.36	4.03	4.1	0.119	1.483	2.836
${}_{1,2}Li_{1,2}^-$		8.059 016	3.92	4.75		0.062	0	4.219
${}_1Be_{1,2}^+$	15.041 1	15.035 639	4.77	5.48	5.5	0.220	0.829	1.599
${}_{1,2}Be_{1,2}$		15.415 912	6.68	7.69		0.386	0	2.111
${}_{1,2}Be_{1-3}^-$			Autoionizes					
${}_{1,2}B_{1,2}^+$		25.281 504	8.75	9.80		0.897	0	1.437
${}_{1,2}B_{1-3}$		25.357 510	9.7	10.9		0.056	1.881	4.655
${}_{1-3}B_{1-3}^-$		25.380 955	9.97	11.33		0.036	0	7.042
${}_{1,2}C_{1-3}^+$		37.918 751	12.8	14.3		0.104	1.070	2.726
${}_{1-3}C_{1-3}$		38.090 383	14.6	16.5		0.176	0	3.684
${}_{1-3}C_{1-4}^-$			Autoionizes					
${}_{1-3}N_{1-3}^+$		53.528 203	18.7	20.9		0.400	0	2.557
${}_{1-3}N_{1-4}$		53.569 533	19.1	21.5		0.031	2.423	7.139
${}_{1-4}N_{1-4}^-$		53.582 040	19.3	21.7		0.030	0	11.094
${}_{1-3}O_{1-4}^+$		71.836 884	23.8	26.6		0.059	1.382	4.267
${}_{1-4}O_{1-4}$		71.929 302	24.9	28.1		0.098	0	5.806
${}_{1-4}O_{1-5}^-$			Autoionizes					
${}_{1-4}F_{1-4}^+$		93.125 365	30.5	34.2		0.217	0	4.048
${}_{1-4}F_{1-5}$		93.149 851	30.7	34.5		0.020	2.939	10.041
${}_{1-5}F_{1-5}^-$		93.157 319	31	35		0.037	0	15.538
${}_{1-4}Ne_{1-5}^+$		117.256 746	36.3	40.9		0.037	1.745	6.246
${}_{1-5}Ne_{1-5}$		117.312 529	37	42		0.067	0	8.586
${}_{1-5}Ne_{1-6}^-$			Autoionizes					

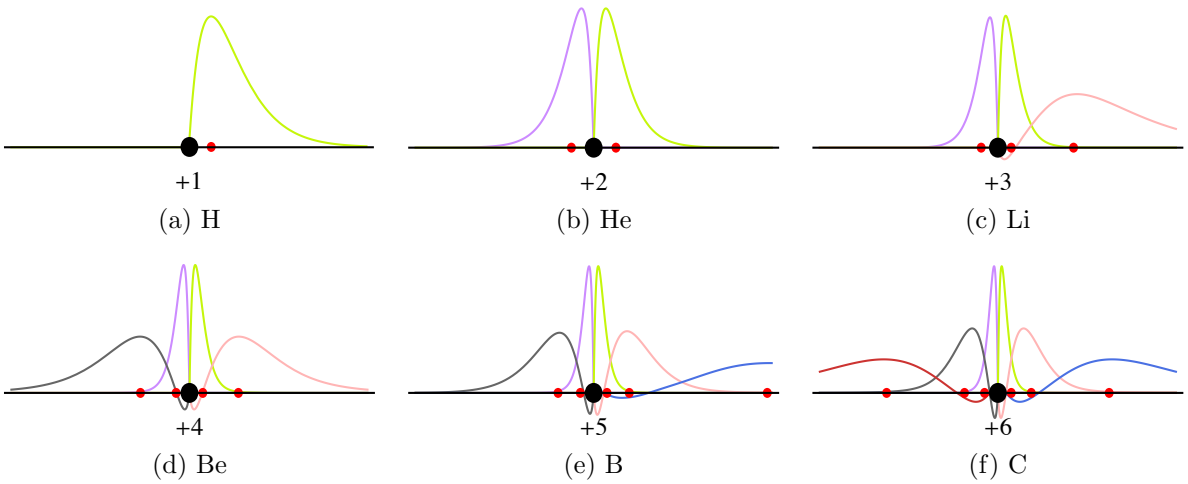

(a) H (b) He (c) Li

(d) Be (e) B (f) C

FIG. 2. HF ground state orbitals of the H, He, Li, Be, B and C atoms. The positions of the nucleus are represented by the black dots while the most likely position of the electrons are represented by red dots.

TABLE III. Ionization energy and electron affinity (in eV) of 1D atoms

Atom	Ionization energy $A \longrightarrow A^+ + e^-$			Electron affinity $A + e^- \longrightarrow A^-$		
	HF	MP2	MP3	HF	MP2	MP3
H	13.606	13.606	13.606	3.893	3.939	3.961
He	33.822	33.878	33.895	0	0	0
Li	4.486	4.517	4.522	1.395	1.410	1.414
Be	10.348	10.400	10.408	0	0	0
B	2.068	2.09	2.098	0.643	0.651	0.655
C	4.670	4.719	4.733	0	0	0
N	1.125	1.14	1.14	0.340	0.35	0.35
O	2.515	2.54	2.56	0	0	0
F	0.666	0.67	0.67	0.203	0.21	0.2
Ne	1.518	1.5	1.5	0	0	0

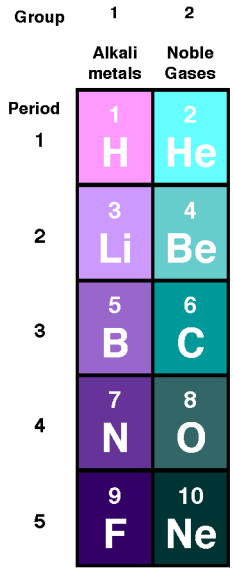

FIG. 3. Periodic table in 1D

TABLE IV. Structures (in a.u.), total energies (in E_h), correlation energies (in mE_h), gaps (in E_h) and vibrational frequencies ν (in cm^{-1}) of 1D molecules

	Molecule		Total energy		Correlation energy			Gap	ν
	State	Bond length	$-E_{\text{exact}}$	$-E_{\text{HF}}$	$-E_c^{\text{MP2}}$	$-E_c^{\text{MP3}}$	$-E_c$		
One-electron diatomics	H_1H^+	$R_{\text{eq}} = 2.581$	0.830 710	0.830 710	0	0	0	3.42	2470
	He_1H^{2+}	$R_{\text{eq}} = 2.182$	1.830 303	1.830 303	0	0	0	2.39	3553
		$R_{\text{ts}} = 3.296$	1.809 411	1.809 411	0	0	0	1.28	1914
	He_1He^{3+}	$R_{\text{eq}} = 1.793$	1.986 928	1.986 928	0	0	0	9.89	4267
		$R_{\text{ts}} = 4.630$	1.694 543	1.694 543	0	0	0	1.48	1028
Two-electron diatomics	H_1H_1	$R_{\text{eq}} = 2.639$	1.185 948	1.184 571	0.846	1.156	1.377	0.264	2389
	$_1He_1H^+$	$R_{\text{eq}} = 2.016$	3.444 390	3.441 957	1.715	2.203	2.433	1.220	3747
	$He_1H_1^+$	$R_{\text{eq}} = 2.037$	2.517 481	2.516 810	0.455	0.595	0.671	0.443	3939
	$He_1He_1^{2+}$	$R_{\text{eq}} = 1.668$	4.112 551	4.110 780	1.275	1.620	1.771	1.480	4755
		$R_{\text{ts}} = 3.989$	3.807 432	3.807 165	0.164	0.222	0.267	0.307	1286
Triatomics	$H_1H_1H^+$	$R_{\text{eq}} = 2.664$	1.570 720	1.569 820	0.582	0.778	0.900	1.557	1178[a]

[a]Symmetric vibrational mode.

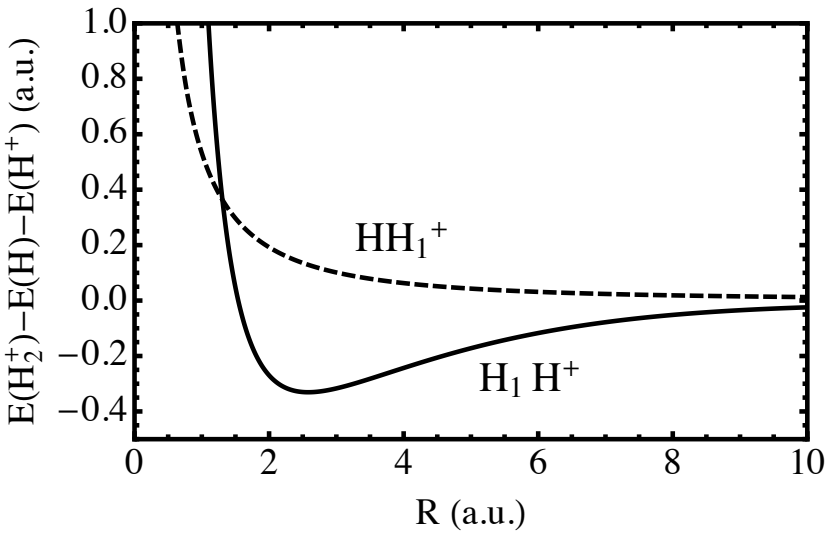

FIG. 4. Potential energy curves of the H_1H^+ and HH_1^+ states of H_2^+

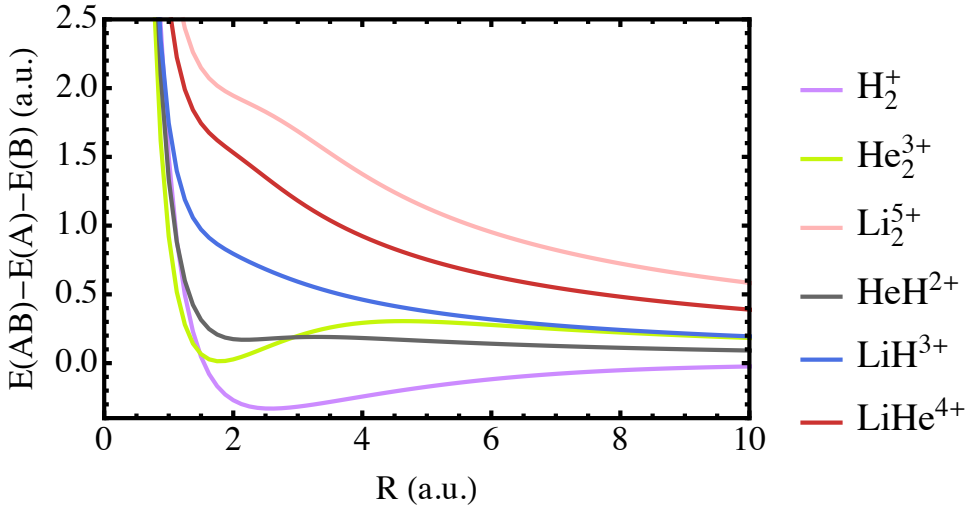

FIG. 5. Potential energy curves of the $A_1B^{Z_A+Z_B-1}$ states of several one-electron diatomics

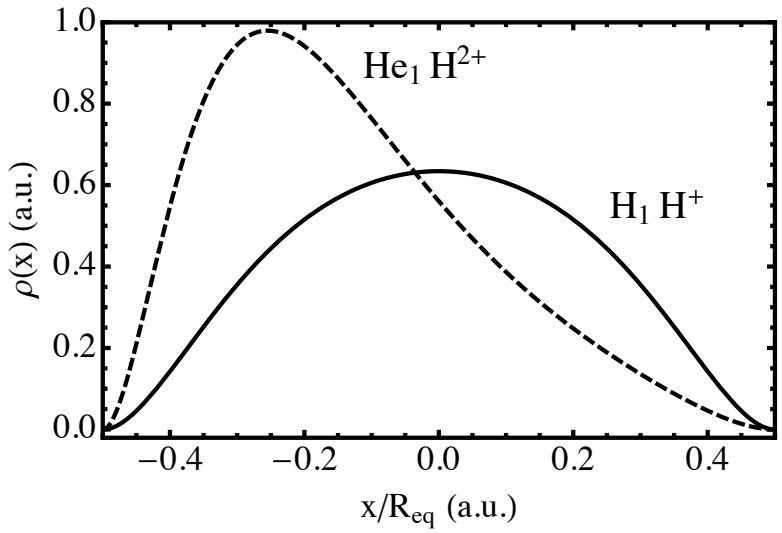

FIG. 6. Electronic density $\rho(x)$ in H_1H^+ and He_1H^{2+} at their equilibrium bond lengths

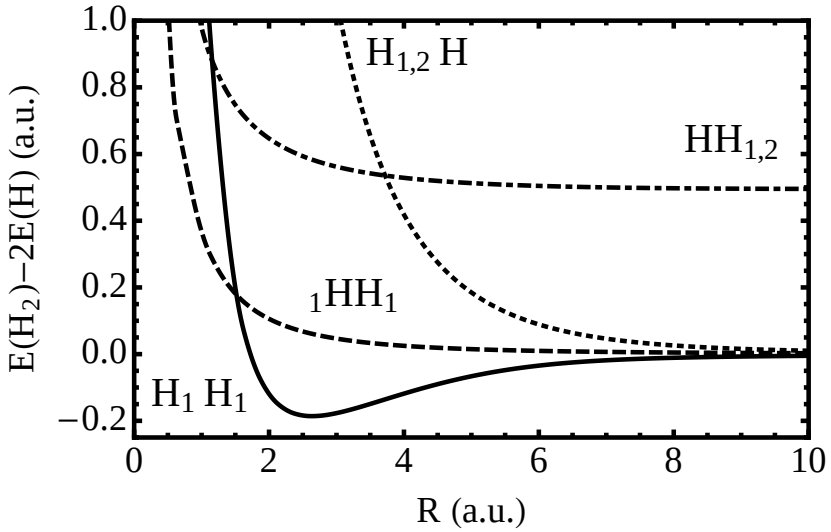

FIG. 7. Potential energy curves of the H_1H_1, $_1HH_1$, $H_{1,2}H$ and $HH_{1,2}$ states of H_2

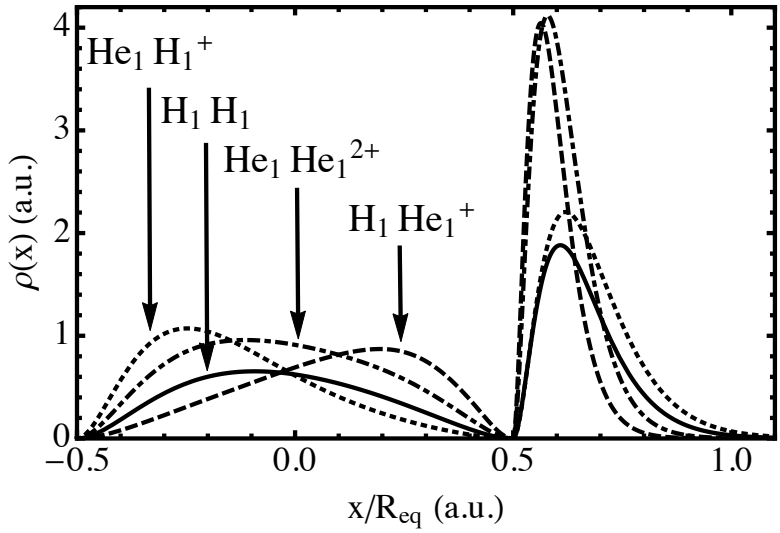

FIG. 8. Electronic density $\rho(x)$ in H_1H_1, $H_1He_1^+$, $He_1H_1^+$ and $He_1He_1^{2+}$ at their equilibrium bond lengths